HIGH-RESOLUTION RADAR IMAGES OF MERCURY FROM THE 2019 INFERIOR CONJUNCTION.

E. G. Rivera-Valentín[1], S. S. Bhiravarasu[1], H. M. Meyer[1], P. A. Taylor[1], M. C. Nolan[2], N. L. Chabot[3], A. K. Virkki[4], [1]Lunar and Planetary Institute, USRA, Houston, TX, [2]Lunar and Planetary Laboratory, Univ. of Arizona, Tucson, AZ, [3]Johns Hopkins University Applied Physics Laboratory, Laurel, MD, [4]Arecibo Observatory, UCF, Arecibo, PR.

Introduction: Radar is a powerful tool to constrain the near-surface, wavelength-scale properties of planetary bodies. Previous ground-based radar imaging campaigns of Mercury revealed radar-bright features consistent with volume backscatter from a low-loss volatile, such as clean water ice, located largely within polar impact craters [1-3]. The MESSENGER spacecraft confirmed that polar radar-bright features are associated with locations permanently in shadow [4, 5] that are on average hydrogen-rich [6]. Additionally, early Arecibo radar data from the mid-latitudes revealed the prominence and variety of fresh impact craters and their ray systems [7]. This included the discovery of several rayed impact craters, such as Hokusai.

Here we report on our recent Mercury radar observations using the Arecibo Observatory in Puerto Rico. Since the early observations (e.g., [2, 3, 7, 8]), Arecibo has gone through several upgrades, allowing for improved spatial resolution; however, damage due to Hurricane Maria has reduced the antenna gain at S band, affecting signal-to-noise ratio. Our work here concentrates on four distinct features: Fonteyn, Hokusai, and Rachmaninoff craters, and the north polar region.

Observations: We conducted monostatic observations of Mercury using the Arecibo S-band (12.6 cm) planetary radar system during inferior conjunction in July 2019 (see Table 1). The subradar latitude allowed for observations of only the north pole. The antenna beam width at S band is larger than Mercury's angular width; therefore, the north-south ambiguity, which superimposes topography from similar latitudes in the northern and southern hemisphere, cannot be avoided. We used the long-code delay-Doppler radar imaging method [9] with a baud of 5 μs (i.e., 750 m/pixel resolution in the delay dimension) to eliminate Doppler aliasing of the slightly overspread target. Echoes in both the opposite circular (OC) and same circular (SC) polarization as transmitted were recorded.

Table 1. Observation conditions.

Date	Subradar Latitude	Subradar Longitude	1-way Light Time
07/19/19	11.50 °N	299.51 °W	4.79 min
07/20/19	11.55 °N	306.34 °W	4.81 min
07/21/19	11.57 °N	313.18 °W	4.83 min
07/22/19	11.56 °N	320.01 °W	4.86 min
07/23/19	11.53 °N	326.83 °W	4.90 min
07/24/19	11.46 °N	333.62 °W	4.95 min

Radar Analysis: Delay-Doppler radar images for each polarization were calibrated then transformed to a simple cylindrical equidistant projection with a resolution of 0.25° for the mid-latitudes and a stereographic projection for the polar terrain following standard techniques [10,11]. The final maps were georeferenced with prominent features using MESSENGER's Mercury Dual Imaging System (MDIS) maps to adjust to hermiocentric coordinates. Although the north-south ambiguity exists for Mercury, all data were mapped onto the northern hemisphere. Here we show OC and SC radar backscatter images that are z-score normalized with respect to the area shown (Fig. 1).

Fonteyn crater (32.8°N, 264.4°W): In the mid-latitudes, Fonteyn crater (diameter of D=29 km) is the most prominent feature. It appeared radar bright in both OC and SC over a range of incidence angels ($40° < \theta < 60°$) from July 19 - 22. The crater floor is relatively darker than the radar-bright, continuous ejecta of this fresh crater owing to the relatively smoother (at S band wavelengths) crater floor compared to the blocky, rough ejecta. Although rays are discernible in MDIS data, there is no accompanying distinct radar signature.

Hokusai crater (58.3°N, 342.3°W): The rayed crater Hokusai (D=95 km) is visually distinguishable on Mercury with rays extending well into the southern hemisphere. It was first observed as "Feature B" in early Arecibo radar images [7, 12]. Here, the rays are clearly visible in both the OC and SC images. Since this region is observed at a high incidence angle, power in OC results from radar-facing slopes (e.g., the bright spots at the bottom of the image), as well as diffuse scattering from wavelength-scale roughness, while power in SC results from diffuse scattering from wavelength-sized scatterers. As such, the high power in both OC and SC returns for Hokusai is a result of both rough terrain and fresh, blocky ejecta [13].

Rachmaninoff crater (27.7°N, 302.6°W): The peak ring crater Rachmaninoff (D=290 km) is readily observable in OC images, but nearly indiscernible in SC radar images. At the observed low incidence angle, the radar return is dominated by quasi-specular scattering from smooth surfaces and radar-facing slopes. Indeed, the interior of Rachmaninoff is reported to be primarily young (<1 Ga) smooth plains caused by impact melt and/or volcanism [14], which is consistent with our radar observations of smooth interior deposits surrounded by radar-facing slopes.

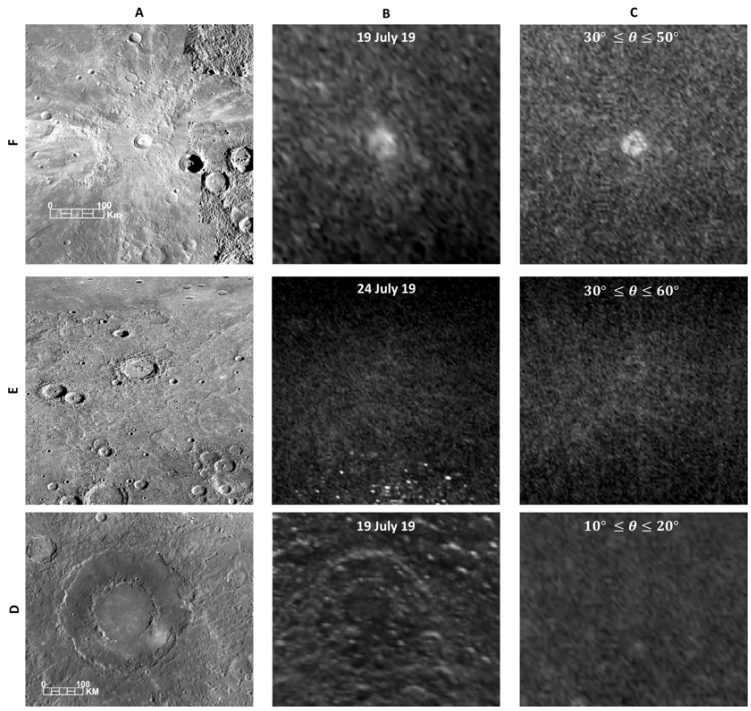

Figure 1: MESSENGER MDIS data (column A) with accompanying simple cylindrical equidistant map projected delay-Doppler radar images (columns B & C) for the three studied craters: Fonteyn (row F), Hokusai (row E), and Rachmaninoff (row D). OC data is in column B and SC data is in column C. The observation date for the radar data is shown at the top of images in column B while the range for the incidence angles in each radar image is shown at the top of images in column C. Radar data is z-score normalized (i.e., such that the average of the pixel values in the image is zero with a standard deviation of one) with respect to the area shown; the color scale, where bright colors represent radar bright regions in the respective polarization, is scaled the same for all craters. MESSENGER MDIS data used here is from https://messenger.quickmap.io

North Polar Region: The observed radar-bright regions in Mercury's north pole agree spatially with previous observations [1-3, 8], and the locations of craters permanently in shadow [5], including the most striking deposits on the floors of Prokofiev, Kandinsky, Tolkien, Chesterton, and Tryggvadóttir (Fig. 2), with abundant smaller deposits also evident. Thus, the craters have retained stable water ice at least over two decades. Indeed, the deposits may be some 300 Myr old [15]. Recent analysis shows, though, that not all craters able to host ice have an accompanying significant radar return [16]. Possible explanations include: (1) a lack of water ice in these regions, and thus not all cold-traps are occupied, (2) incomplete longitudinal coverage by the radar measurements, (3) thin water ice deposits that do not cause a strong enough radar return, or (4) water ice buried below the radar penetration depth. Our new data will allow us to conduct higher-order, radar scattering analysis in order to provide constraints on these possibilities.

References: [1] Slade, M. A. et al. (1992) Science 258, 635-640. [2] Harmon, J. K. & Slade, M. A. (1992) Science, 258, 640-643. [3] Harmon, J. K. et al. (1994) Nature 369, 213-215. [4] Chabot, N. L. et al. (2012) GRL 39, L09204. [5] Deutsch, A. N. et al (2016) Icarus 280, 158-171. [6] Lawrence, D. J. et al. (2013) Science 339, 292-296. [7] Harmon, J. K. et al. (2007) Icarus 187, 374-405. [8] Harmon, J. K. et al. (2011) Icarus 211, 37-50. [9] Harmon, J. K. (2002) IEEE Trans. G&RS 40, 1904-1916. [10] Pettengill, G. H. et al. (1974) The Moon, 10, 3-16. [11] Campbell, B. A. (2002) Cambridge Univ. Press. [12] Harmon, J. K. (1997) Adv. Space Sci. 19, 1487-1496. [13] Neish, C. D. et al. (2013) JGR Planets 118, 2247-2261. [14] Prockter, L. M. et al. (2010) Science 329, 668-671. [15] Deutsch, A. N. et al. (2019) Icarus 520, 26-33. [16] Chabot, N. L. et al. (2018) JGR Planets 123, 666-681.

Acknowledgements: This research was supported by NASA through NEOO under Grant No. NNX13AQ46G (PI: P. A. Taylor) and SSO under Grant No. 80NSSC19K0523 (PI: A. K. Virkki). The Arecibo Observatory is a facility of the NSF managed under cooperative agreement by UCF in alliance with Yang Enterprises, Inc., and Ana G. Méndez University.

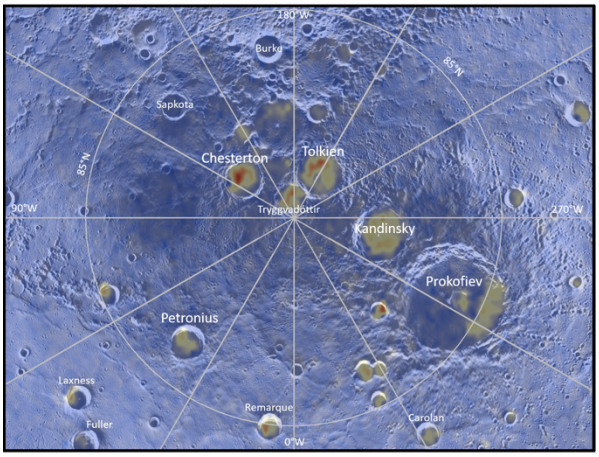

Figure 2: Stereographic projection of the north pole with radar data overlain on an MDIS mosaic. Here, radar return is the sum of OC and SC backscatter, where redder shades indicate higher values.